Free-Electron Lasing without Inversion by Interference of Momentum States

G. Kurizki
Department of Chemical Physics, Weizmann Institute of Science, Rehovot 76100, Israel

M. O. Scully
Department of Physics, Texas A&M University, College Station, Texas 77843

C. Keitel
Optics Section, The Blackett Laboratory, Imperial College, London SW7 2BZ, United Kingdom
(Received 2 October 1992)

It is shown that lasing in free-electron devices can be attained without the standard population inversion between the two portions of the electron momentum distribution that contribute to simulated emission and absorption, respectively. Coherent superpositions of two electronic states in appropriately designed wigglers can strongly suppress stimulated absorption without hampering stimulated emission. The resulting gain curve is symmetric about the emission resonance, and yields a much larger gain than the antisymmetric gain curve of a standard free-electron laser with the same parameters.

PACS numbers: 41.60.Cr, 52.75.Ms

Free-electron lasers (FELS) owe their gain to the fact that, in the quantum description, an electron recoils in opposite directions depending on whether it emits or absorbs a photon with a given wave vector $\mathbf{q}$. Hence, the resonant electronic momentum $\hbar\mathbf{k}_e$ for the emission of such a photon differs from the resonant momentum $\hbar\mathbf{k}_a$ for its absorption. This leads to the gain-spread theorem [1-4], which expresses (in the simple one-dimensional case) the small-signal gain as the convolution of the electron momentum distribution $f(k)$ with the difference between the probability distributions (line shapes) of emission and absorption per photon, which are centered at k_e and k_a, respectively. Hence, when these line shapes are much narrower than the spread of $f(k)$, the small-signal gain is proportional to the "population inversion" $f(k_e) - f(k_a)$. In the quasiclassical limit, which holds when $k_e - k_a$ is much smaller than the inverse length of the wiggler, and the photon energy $\hbar cq$ is much smaller than the electron energies $E(k_{e(a)})$, the small-signal gain curve is *antisymmetric* about the mean resonant momentum $\hbar\bar{k} = \hbar(k_e + k_a)/2$. The resulting gain is then proportional to the product of the following factors [2]: (a) the small photon-recoil factor $\hbar cq/E$; (b) the emission rate per photon, $P(q)/\hbar cq$, where $P(q)$ is the corresponding emission power; and (c) the derivative of the momentum distribution at $\bar{k}$, $df(k)/dk|_{\bar{k}}$. In this limit, the quantum expression for gain coincides with its classical counterpart, which follows from the momentum bunching of the electrons by the interaction [5,6].

The shape of the FEL gain curve and its dependence on photon recoil and the momentum distribution of nearly free electrons stand in sharp contrast to the corresponding features in lasers operating between discrete electronic states in atoms, whose gain curves are *symmetric* about the atomic resonance and are nearly independent of photon recoil. In view of these fundamental differences, one may ask if it is possible and worthwhile to implement in FELs a mechanism analogous to that of atomic lasing without inversion (LWI), whereby the role of *population inversion is replaced by coherence* between two electronic states [7-9]. We hope to convince the reader that the answer is yes.

In this Letter we show, for the first time, that it is possible, in principle, to attain LWI in free-electron devices. This mode of operation can render the gain curve symmetric about the emission resonance, broaden the gain profile, and bring about strong enhancement of the maximal small-signal gain. The broadening of the gain curve and the gain enhancement can relax the requirements on the electron beam at lasing threshold, and thereby help the attainment of x-ray lasing in electromagnetic wigglers (Compton scattering from laser pump beams) [1,10,11]. In the scheme considered, the electron interacts with the FEL signal in two different regions with different vectorial momenta whose amplitudes add up coherently. Likewise, the wiggler is characterized by a superposition of two beams with differently oriented wave vectors. Photon absorption from the FEL signal can then be arranged to proceed via two interfering near-resonant channels leading to a common final state of the electron. When the phases of the channel amplitudes make them interfere destructively, stimulated absorption is practically eliminated, since the other channels of absorption are far from resonance. In contrast, each of the corresponding electronic states obtained by near-resonant stimulated emission is accessed via a single channel, so that the population of these states is unaffected by interference. Gain enhancement then results, because the rate of simulated emission is similar to that of conventional FELs, whereas stimulated absorption is strongly suppressed. We note that two-channel interference leading to either enhanced or suppressed population of *electron-momentum states* has been proposed for the coherent control of photocurrents in semiconductors [12] or the detection of squeezed light [13].

Let us first review the kinematics of single-photon absorption and emission in the ordinary noncollinear FEL scheme [2]. Consider one of the solid lines in the paraboloid of energy-momentum dispersion [Fig. 1(a)] marking the absorption of a signal photon with wave vector $\mathbf{q}=(\omega/c)\hat{\mathbf{z}}$ by an electron with momentum $\hbar\mathbf{k}_1$ or $\hbar\mathbf{k}_2$ and energy

$$E=[(\hbar c k_{1(2)})^2+m^2c^4]^{1/2} \tag{1}$$

in the presence of an optical or magnetic wiggler with wave vector $\mathbf{k}_{w1}$ or $\mathbf{k}_{w2}$, respectively. The absorbed photon takes the electron vertically up from the E plane to the plane of $E_a=E+\hbar\omega$. A momentum "kick" corresponding to wiggler-photon emission results in a final electron momentum,

$$\mathbf{k}_{a1(2)}=\mathbf{k}_{1(2)}-\mathbf{k}_{w1(2)}+\mathbf{q}\,, \tag{2}$$

which must lie near the "resonant," i.e., kinematically allowed, upper circle on the paraboloid surface. The detuning (momentum mismatch) Δ_a, corresponding to the radial distance of $\mathbf{k}_a$ from this circle, can be varied by changing either one of the momenta on the right-hand side of Eq. (2). The same considerations determine the detuning Δ_e of the final electron state accessed by signal-photon emission (via one of the dashed lines) from the resonant-momentum value

$$\mathbf{k}_{e1(2)}=\mathbf{k}_{1(2)}+\mathbf{k}_{w1(2)}-\mathbf{q}\,. \tag{3}$$

The standard gain G_s, to first order in the signal intensity, is proportional to the difference between the transition rates for emission band absorption, convoluted with the initial distribution of electron momenta $f(\mathbf{k})$:

$$G_s \propto \int [\mathrm{sinc}^2(\Delta_e L/2)-\mathrm{sinc}^2(\Delta_a L/2)]f(\Delta)d\Delta\,, \tag{4}$$

where L is the interaction length and $\Delta_{e(a)}=\Delta\mp\epsilon/2$, ϵ being determined by the difference between the photon recoil in Eq. (2) and its counterpart in Eq. (3). In the limit of small recoil $\epsilon L\ll 1$, the gain profile within the square brackets of Eq. (4) is almost antisymmetric about $\Delta=0$, resulting in a very weak gain for a broad, nearly symmetric $f(\Delta)$.

In order to improve the standard gain performance, we arrange the electron-laser interaction to occur in two sequential regions involving electron states $|\mathbf{k}_1\rangle$ and $|\mathbf{k}_2\rangle$, and the wiggler in a superposition of $\mathbf{k}_{w1}$ and $\mathbf{k}_{w2}$ modes. In this way we can impose conditions for destructive interference of the absorption channels. To this end, consider Fig. 1(b), wherein an electron beam is collimated to a width $w_e\gg k_w^{-1}$ having a mean momentum $\hbar\mathbf{k}_1=\hbar k\times[\cos\phi\hat{\mathbf{z}}-\sin\phi\hat{\mathbf{x}}]$. This beam interacts in region 1, centered at $\mathbf{r}_1=(-\bar{z},\bar{x})$, with a wiggler beam of width $L\geq w_e$, and mean wave vector $\mathbf{k}_{w1}=k_w[\cos(\pi-\theta)\hat{\mathbf{z}}-\sin\theta\hat{\mathbf{x}}]$. The nonscattered part of the electron beam is deflected (magnetically or electrostatically) at an angle ϕ, thereby acquiring a momentum $\hbar\mathbf{k}_2=\hbar k[\cos\phi\hat{\mathbf{z}}+\sin\phi\hat{\mathbf{x}}]$. It then interacts in region 2, centered at $\mathbf{r}_2=(+\bar{z},\bar{x})$, with another wiggler beam of width L and

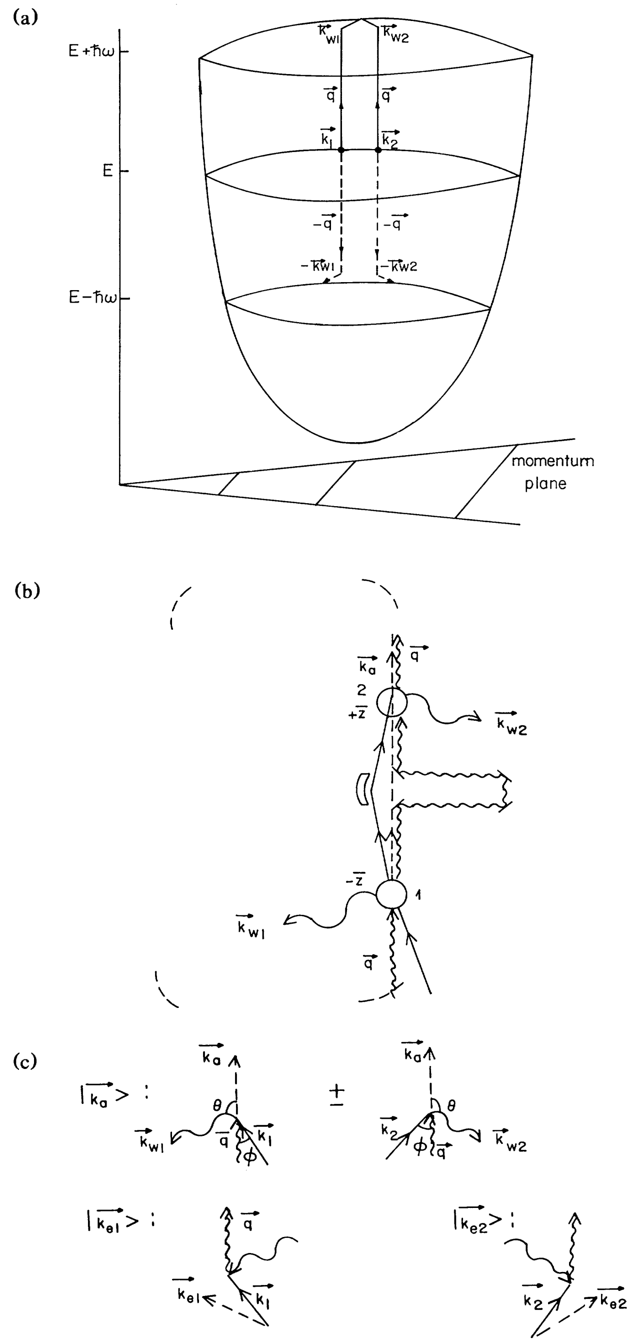

FIG. 1. (a) Kinematics of photon absorption (solid lines) and emission (dashed lines) by two differently oriented electron and wiggler momenta, leading to a common final state in absorption and orthogonal states in emission. (b) Realization of this scheme in two sequential interaction regions (1 and 2) with *interfering* scattering amplitudes into state $|\mathbf{k}_a\rangle$ via absorption of signal photon $\mathbf{q}$. The required signal delay is achieved either by a ring resonator (dashed lines for mirrors) or a four-mirror deflector (between regions 1 and 2). (c) Feynman diagrams for absorption into $|\mathbf{k}_a\rangle$ by the two constructively or destructively interfering interaction channels (+ or − signs), and for emission, leading to orthogonal states $|\mathbf{k}_{e1}\rangle$ and $|\mathbf{k}_{e2}\rangle$.

mean wave vector $\mathbf{k}_{w2}=k_w[\cos(\pi-\theta)\hat{\mathbf{z}}+\sin\theta\hat{\mathbf{x}}]$. The interaction regions 1 and 2 are isolated as long as $2\bar{z}\gg L\geq w_e$. The wiggler is represented by the vector potential

$$\mathbf{A}_w=\hat{\mathbf{y}}[a_{w1}g(z+\bar{z},x-\bar{x})|\mathbf{k}_{w1}\rangle + a_{w2}g(z-\bar{z},x-\bar{x})|\mathbf{k}_{w2}\rangle]\,, \tag{5}$$

where the g's are the localization functions and $a_{w1(2)}=|a_{w1(2)}|\exp(i\alpha_{1(2)})$ are the beam amplitudes (treated here classically). Both wiggler beams are derived from the same coherent source, and hence the phase difference $\alpha_1-\alpha_2$ is fixed. The signal, after interacting with the electron in region 1, must be delayed by a distance D, so that it reaches region 2 *simultaneously* with the electron. This can be done in one of the following ways [Fig. 1(b)]: (a) by enclosing both interaction regions in a ring resonator for the signal, which can then make one or more round trips in the resonator on its way between the regions; (b) by deflecting the signal sideways from the z axis and back again, by a four-mirror configuration.

Absorption of the signal photon in regions 1 and 2 will scatter the electron into a *common* final state $|\mathbf{k}_a\rangle$ if

$$\mathbf{k}_a\approx\mathbf{k}_1-\mathbf{k}_{w1}+\mathbf{q}=\mathbf{k}_2-\mathbf{k}_{w2}+\mathbf{q}\,, \tag{6a}$$

which requires

$$\sin\phi=(k_w/k)\sin\theta\,. \tag{6b}$$

This is a necessary condition for interference in absorption. By contrast, $|\mathbf{k}_{e1}\rangle$ and $|\mathbf{k}_{e2}\rangle$ in Eq. (3) are then *strongly orthogonal*, with a momentum mismatch of

$$|\mathbf{k}_{e1}-\mathbf{k}_{e2}|\approx 4k_w\sin\theta=4k\sin\phi\,, \tag{7}$$

whence there is no interference in emission.

Consider next the resulting state of the electron as it passes through the FEL in Fig. 1(b). As illustrated in Fig. 1(c), the final state of the electron $|f\rangle$ after interacting with the signal in both regions is given by

$$|f\rangle\cong|i\rangle+(c_{a2}+c_{a1})|\mathbf{k}_a\rangle+c_{e2}|\mathbf{k}_{e2}\rangle+c_{e1}|\mathbf{k}_{e1}\rangle\,. \tag{8a}$$

Here the "initial" (nonscattered) part of the electron state is a sum of the incident and deflected beams, weighted by their amplitudes c_1 and c_2:

$$|i\rangle=c_1\psi(\mathbf{r}-\mathbf{r}_1)|\mathbf{k}_1\rangle\quad(z<0)$$
$$+c_2\psi(\mathbf{r}-\mathbf{r}_2)|\mathbf{k}_2\rangle\quad(z>0)\,, \tag{8b}$$

where $\psi(\mathbf{r}-\mathbf{r}_{1(2)})$ describe the electron-beam localization within w_e, and the phases of $c_{1(2)}$ account for the propagation from region 1 to region 2. Under the conditions of Eq. (6), the absorption part of the electron state is given by the second term in Eq. (8a), where c_{a1} (c_{a2}) is the probability amplitude for the electron to absorb the signal photon in the first (second) region. The amplitudes c_{e1} and c_{e2} are the emission scattering amplitudes in the respective regions. The main point is that c_{a2} and c_{a1} can be arranged to interfere, in this scheme, which bears analogy to *atomic Ramsey-fringe schemes.* By contrast, c_{e2} and c_{e1} cannot interfere, because of the orthogonality of $|\mathbf{k}_{e1}\rangle$ and $|\mathbf{k}_{e2}\rangle$ [Eq. (7)].

Let us now proceed to calculate the probability amplitudes for absorption ($c_{a1(2)}$) and emission ($c_{e1(2)}$) of a y polarized signal photon in this scheme. The interaction Hamiltonian can be effectively reduced to [2]

$$H_I\approx e(\mathbf{A}_s+\text{H.c.})\cdot(\mathbf{p}-e\mathbf{A}_w+\text{H.c.})/m\gamma$$
$$\approx e^2(\mathbf{A}_s+\text{H.c.})(\mathbf{A}_w+\text{H.c.})/m\gamma\,, \tag{9}$$

where the signal vector potential is $\mathbf{A}_s=\hat{\mathbf{y}}a_s\exp(iqz)$, $\mathbf{p}$ is the electron momentum, and $m\gamma$ is the relativistic mass. As is well known [2], the $\mathbf{p}\cdot\mathbf{A}$ term is negligible when $\mathbf{k}_{1(2)}$ are nearly aligned with $\hat{\mathbf{z}}$ (see ϕ values below) and have no y component. The rotating-wave approximation (RWA) terms $A_s^\dagger A_w$ and $A_sA_w^\dagger$ are predominant in near-resonant emission and absorption, since their respective momentum detunings Δ_e and Δ_a are much smaller than those of non-RWA terms A_sA_w and $A_s^\dagger A_w^\dagger$, which are detuned from resonance by $\sim k_w\gg|\Delta_{e(a)}|$ (see below).

When the condition for interference in absorption [Eq. (6)] holds, the corresponding RWA transition probability becomes proportional to the square of

$$\langle\mathbf{k}_a|A_sA_w^\dagger|i\rangle=c_{a1}^*+c_{a2}^*=a_s\int d\mathbf{r}[c_1a_{w1}^*\psi(\mathbf{r}-\mathbf{r}_1)g(\mathbf{r}-\mathbf{r}_1)+\tilde{c}_2a_{w2}^*\psi(\mathbf{r}-\mathbf{r}_2)g(\mathbf{r}-\mathbf{r}_2)]$$
$$\times\exp[-i(\mathbf{k}_a-\mathbf{q}+\mathbf{k}_{1(2)}-\mathbf{k}_{w1(2)})\mathbf{r}]\,. \tag{10}$$

Absorption will be effectively canceled when $c_1a_{w1}^*=-\tilde{c}_2a_{w2}^*$, where $\tilde{c}_2=c_2\exp[i(2\bar{z}+D)q]$ includes the signal phase shift along its delay path D (discussed above). By contrast, the RWA emission probability is given by a sum of two noninterfering contributions,

$$P_e\propto|\langle\mathbf{k}_{e1}|A_s^\dagger A_w|i\rangle|^2+|\langle\mathbf{k}_{e2}|A_s^\dagger A_w|i\rangle|^2=|c_{e1}|^2+|c_{e2}|^2\propto\text{sinc}^2(\Delta_eL)\,, \tag{11}$$

as implied by Eq. (7). Thus, the cancellation of absorption *does not change the emission probability* P_e, whose line shape is symmetric in the emission detuning Δ_e.

We can now write down the ratio of the absorption-free gain G_{AF}, which is simply proportional to P_e, to the standard gain G_s [Eq. (4)], evaluated for the same parameters (current density, wiggler power density, wiggler and electron momenta, and interaction length),

$$\frac{G_{\text{AF}}}{G_s}\approx\frac{\sin^2(\frac{1}{2}\Delta_eL)/(\frac{1}{2}\Delta_e)^2}{\sin^2[\frac{1}{2}(\Delta-\epsilon)L]/[\frac{1}{2}(\Delta-\epsilon)]^2-\sin^2[\frac{1}{2}(\Delta+\epsilon)L]/[\frac{1}{2}(\Delta+\epsilon)]^2}\,. \tag{12}$$

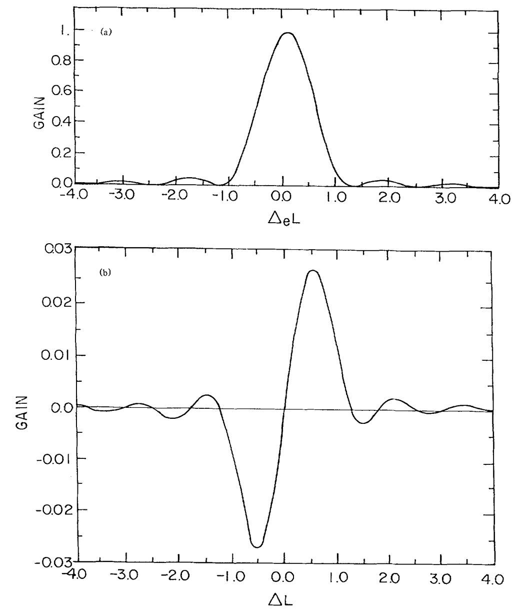

FIG 2. Gain profiles as a function of (a) $\Delta_e L$ for the absorption-free scheme (maximal gain is 1.0) and (b) ΔL for the standard FEL (maximal gain is 0.025), using the same parameters ($\epsilon=0.01$).

For $\epsilon\approx 0.01$, typical of the photon recoil due to hard x-ray emission in an optical wiggler [7,8], $G_{\rm AF}/G_s\approx 40$ is attainable at their respective maxima (Fig. 2). The gain curve $G_{\rm AF}$ is seen to be symmetric about the emission resonance, as opposed to the nearly antisymmetric G_s. The resonant condition $\Delta_e=0$ corresponds to the following resonant emission frequency ω_e, obtainable from Eqs. (1) and (3) for $\gamma\gg 1$ and $|\phi|=\hbar k_w|\sin\theta|/mc\gamma\ll 1$:

$$\omega_e\approx 2\gamma^2 ck_w\cos\theta(1-\hbar ck_w/mc\gamma)\,. \tag{13}$$

The frequency is shifted from the resonant absorption frequency ω_a [Eqs. (1) and (2)] by the amount $\sim 2\hbar\times k_w^2\gamma/m$. Curiously, we can tune the signal to ω_a and *still be near the gain maximum,* as long as the corresponding momentum detuning

$$\Delta_e\sim 2\gamma(\hbar k_w^2/mc)\ll L^{-1}\,.$$

The non-RWA terms (see above) would then have $\Delta_{e(a)}L\geq k_wL$, and thus be negligible by comparison.

The predicted gain enhancement can be up to 2 orders of magnitude. This allows the reduction, by the same factor, of the current density $I/\pi w_e^2$, or the wiggler power density required for FEL action. On the other hand, our scheme poses stringent requirements on the angular beam spread $\Delta\phi$, which must satisfy [Eq. (7)] $\gamma\Delta\phi<\hbar k_w\times\sin\theta/mc$. Hence, we should try to work with the largest possible k_w, and thereby maximize the allowed $\Delta\phi$. It may therefore be advantageous to use as a wiggler an intense extreme-UV coherent pulse, presently available by processes such as high-harmonic conversion of excimer-laser pulses in gases [14]. As an example, we can choose a 50 eV wiggler, $\theta\leq\pi/3$ and $\gamma\sim 5$, corresponding to $\hbar\omega_e\approx 2.5$ keV. The required beam spread is then $\Delta\phi\leq 10^{-4}/\gamma$, which is achieved by ~ 1 mm collimators placed ~ 50 m apart.

This first application of the concept of LWI to FELs may pave the way to other such schemes, which can be based on either the quantum or the classical FEL description. Apart from gain enhancement, the main *qualitative* consequences of this scheme are as follows: (a) The scaling of the FEL gain with frequency is now determined by the spontaneous emission rate, rather than by photon recoil, even in the quantum regime. (b) The *inhomogeneous width* of electron energies compatible with gain can now be broader and more symmetric about the emission resonance value, thereby relaxing the required electron-beam monochromaticity. (c) The study of the emitted photon statistics is expected to be of considerable interest, in view of its strong dependence on recoil in the quantum regime of the standard FEL [15].

[1] For an updated comprehensive treatment, see C. Brau, *Free-Electron Lasers* (Academic, Boston, 1990).
[2] For a review of the quantum FEL description, see A. Friedman, A. Gover, G. Kurizki, S. Ruschin, and A. Yariv, Rev. Mod. Phys. **60**, 471 (1988).
[3] J. M. J. Madey, J. Appl. Phys. **42**, 1906 (1970).
[4] R. Bonifacio and M. O. Scully, Opt. Commun. **32**, 291 (1980).
[5] F. A. Hopf, P. Meystre, M. O. Scully, and W. H. Louisell, Phys. Rev. Lett. **37**, 1342 (1976).
[6] S. F. Jacobs, M. O. Scully, M. Sargent III, and H. Pilloff, *Physics of Quantum Electronics* (Addison Wesley, Reading, MA, 1978), Vol. 5.
[7] S. E. Harris, Phys. Rev. Lett. **62**, 1033 (1989); K. J. Boller, A. Imamoğlu, and S. E. Harris, Phys. Rev. Lett. **66**, 2593 (1991).
[8] M. O. Scully, S. Y. Zhu, and A. Gavrielides, Phys. Rev. Lett. **62**, 2813 (1989).
[9] O. Kocherovskaya and Ya. I. Khanin, Pis'ma Eksp. Teor. Fiz. **48**, 581 (1988) [JETP Lett. **48**, 630 (1988)].
[10] *Free Electron Generation of Extreme UV Coherent Radiation*, edited by J. M. J. Madey and C. Pellegrini (AIP, New York, 1984).
[11] J. Gea-Baracloche, G. T. Moore, R. R. Schlicher, M. O. Scully, and H. Walther, IEEE J. Quantum Electron. **23**, 1558 (1987); Nucl. Instrum. Methods Phys. Res., Sect. A **272**, 199 (1988).
[12] G. Kurizki, M. Shapiro, and P. Brumer, Phys. Rev. B **39**, 3435 (1989).
[13] G. Kurizki and M. Shapiro, in *Coherence and Quantum Optics*, edited by J. H. Eberly, L. Mandel, and E. Wolf (Plenum, New York, 1989), Vol. 6; J. Opt. Soc. Am. B **8**, 355 (1991).
[14] Special Issue on Coherent XUV Radiation [J. Opt. Soc. Am. B **4**, (1987)].
[15] W. Becker, M. O. Scully, and M. S. Zubairy, Phys. Rev. Lett. **48**, 475 (1982); Phys. Rev. A **25**, 2200 (1982).